

Geometry and material parameter dependence of InAs/GaAs quantum dot electronic structure

Craig Pryor*

Pryor Consulting, 1279 West Henderson, P.M.B. 221, Porterville, California 93257

(Received 11 December 1998)

We examine the effects of island geometry and material parameters on confined state energies of an InAs/GaAs pyramidal quantum dot calculated using a strain-dependent eight-band $\mathbf{k}\cdot\mathbf{p}$ Hamiltonian. For a truncated pyramidal dot with 101-type sides the electronic confined state energies depend strongly on the base of the pyramid, but are insensitive to the height. The exciton recombination energy is primarily determined by the island volume. This apparent paradox is explained by the change in strain profile with shape, and the fact that truncating a pyramid has a small effect on the volume. For a typical island size, we compute the sensitivity of the electron and hole ground-state energies to variations in 17 different material parameters. The most critical parameters are the InAs Luttinger parameters, γ_1 and γ_3 for which a 10% shift in either one changes the recombination energy by 20 meV. [S0163-1829(99)06927-1]

I. INTRODUCTION

In recent years, there have been great advances in the fabrication of strained quantum dots using Stranski-Krastonov (SK) growth. This technique produces pyramidal islands of strained semiconductor surrounded by a larger band-gap material. This experimental progress has been accompanied by a variety of theoretical treatments of the electronic structure using effective-mass approximations,^{1,2} multiband $\mathbf{k}\cdot\mathbf{p}$ for the valence band,³⁻⁹ multiband $\mathbf{k}\cdot\mathbf{p}$ with coupled conduction and valence bands,¹⁰⁻¹³ and pseudopotentials.¹⁴⁻¹⁶ However, no matter how sophisticated a calculation may be, it is still no better than its inputs, consisting of the dot geometry and the material parameters.

The size and shape of a quantum dot are obviously important for computing the energy levels. Due to the scale invariance of the equations governing elasticity, the strain for a rescaled dot is obtained by simply rescaling the coordinates. In contrast, changing the shape actually alters the strain distribution in and around the island, and in turn the potential felt by the electrons. Thus, the shape of the dot influences the electronic states in an indirect and very complex manner. The effects of dot size have been investigated, but most calculations have considered a fixed shape, which was then scaled up or down in size. Calculations have been done for pyramidal dots with various angles for the side planes,¹⁷ however, all the islands considered were untruncated pyramids, and only a limited range of sizes were considered. Here we shall consider a different region of shape space.

While there have been many different proposals for the InAs island's shape, there is still considerable debate since the extremely small size of InAs islands makes measurements difficult. The 101 geometry is adopted here because it is in some sense the simplest, and it has been the most studied theoretically. In contrast, InP SK islands are sufficiently large that both atomic force microscopy and scanning electron microscopy measurements can resolve the detailed shape, and identify crystal facets.^{18,19} From these measurements it is well established that InP islands form pyramids that are truncated with a 001 plane. The existence of such

island shapes (albeit, in a different material system) naturally leads one to consider the possibility for InAs. In addition, there is indirect evidence for truncated shapes in InAs from the fact that calculated energies provide the best fit to photoluminescence experiments for truncated pyramids.²⁰

The calculated electronic structure also depends on the material parameters employed. These parameters are determined by experiments on bulk materials, and are subject to random and systematic errors. Clearly, if the assumed value of a material parameter is incorrect, the quantum dot calculation will be in error. However, the electronic energy levels are complicated functions of the input parameters, so the parameter with the largest error does not necessarily provide the largest contribution to the error in the electronic energy. Determining the sensitivity to material parameters is vital to determining the reliability of electronic structure calculations.

In this paper, we consider a material system that has received much attention, an InAs island surrounded by GaAs. After briefly outlining the model and calculational methods, we consider the dependence of confined state energies on the island geometry. Then, for an island of typical size and shape, we compute the dependence of the confined state energies on 17 different material parameters.

II. MODEL

The strain was calculated using continuum elasticity theory by minimizing the elastic energy on a cubic grid of $100\times 100\times 100$ sites. Continuum elasticity has an important advantage over atomistic models such as the valence force field (VFF) model.²¹ In order to make quantum-dot calculations feasible, the VFF method is usually simplified to include only two nearest-neighbor interactions.^{8,14} However, two parameters are insufficient to reproduce the three elastic constants necessary for a cubic crystal,²² and the two-parameter VFF method only approximates the bulk elastic properties.²³

After computing the strain, it was used as input to a

TABLE I. Material parameters. Unless otherwise noted, values are taken from Ref. 27. The γ^L 's are the standard Luttinger parameters (as opposed to the modified Luttinger parameters), E_g is the energy gap, Δ is the spin-orbit splitting, E_p is the Kane matrix element, a_g , a_c , a_v , b , and d are deformation potentials, e_{14} is the piezoelectric constant, the C 's are the elastic constants, a is the lattice constant, ϵ_R is the relative dielectric constant, and E_{vbo} is the strain-independent valence-band offset.

Parameter	InAs	GaAs
γ_1^L	19.67	6.85
γ_2^L	8.37	2.1
γ_3^L	9.29	2.9
E_g	0.418 eV	1.519 eV
Δ	0.38 eV	0.33 eV
E_p	22.2 eV	25.7 eV
a_g	-6.0 eV	-8.6 eV ^a
a_c	-6.66 eV	-9.3 eV ^a
a_v	0.66 eV	0.7 eV ^a
b	-1.8 eV	-2.0 eV
d	-3.6 eV	-5.4 eV
e_{14}	0.045 C/m ² ^b	0.159 C/m ² ^b
C_{xxxx}	8.329×10^{11} dyne/cm ²	12.11×10^{11} dyne/cm ²
C_{xyyy}	4.526×10^{11} dyne/cm ²	5.48×10^{11} dyne/cm ²
C_{xyxy}	3.959×10^{11} dyne/cm ²	6.04×10^{11} dyne/cm ²
a	0.60583 nm	0.56532 nm
ϵ_R	15.15	12.53
E_{vbo}	85 meV ^c	

^aRef. 26.

^bRef. 28.

^cSee text, Sec. II.

strain-dependent eight-band $\mathbf{k} \cdot \mathbf{p}$ Hamiltonian,²⁴ including piezoelectric polarization. Derivatives in the Hamiltonian were replaced with differences on the same cubic grid used for the strain calculation, but with unnecessary barrier material sites removed. The largest such grid contained $45 \times 45 \times 30$ sites, requiring the diagonalization of a $500\,000 \times 500\,000$ matrix, equivalent to a variational basis set of 5×10^5 plane waves.

The resulting sparse matrix was diagonalized using the Lanczos algorithm, which is extremely efficient at solving sparse eigenvalue problems,²⁵ and enables the calculations to be performed on an inexpensive pc. It should be noted that the Lanczos algorithm can solve such problems even though the Hamiltonian is not bounded from below. This is because the Lanczos algorithm converges first to the *extremal* eigenvalues, not the minimum.²⁵ The first eigenvalues to converge are the highest valence-band and lowest conduction-band states. Lanczos has the additional advantage that since the matrix is not squared to obtain a positive definite eigensystem, the condition number of the matrix is not reduced as it is in the folded spectrum method.¹⁶

The values used for the various material parameters are given in Table I. In the calculations, all parameters were set to the values corresponding to the local composition. Most parameters are obtained directly from measurements, however a few merit comment. The hydrostatic deformation potentials for the conduction and valence band a_c and a_v , respectively, are difficult to measure and for many materials they have not been measured at all. In contrast, the gap de-

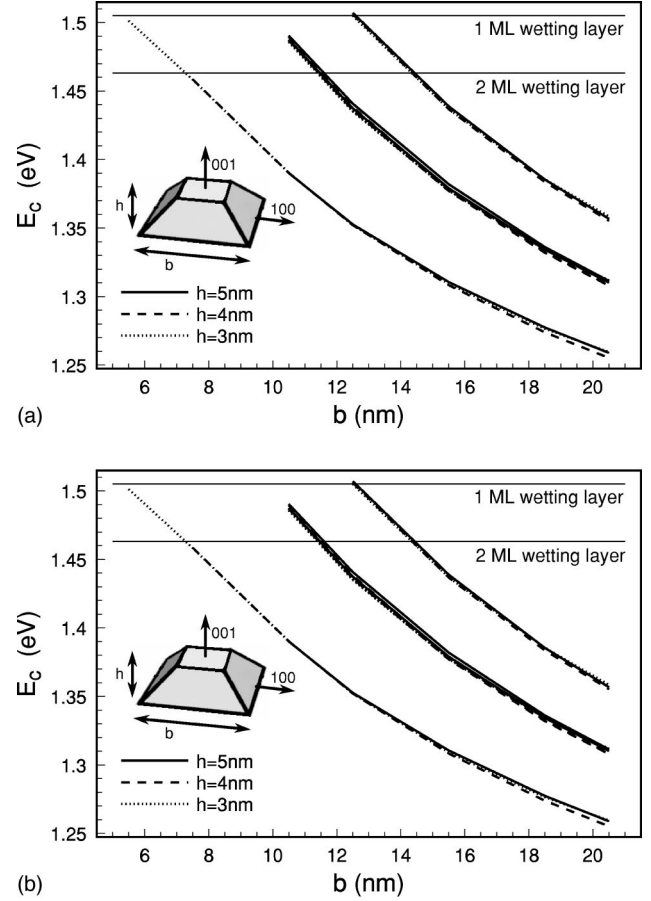


FIG. 1. Confined state energies as a function of the island base, for three different island heights. (a) Conduction band, (b) valence band. Also indicated are the ground-state energies for quantum wells containing 1.5 and 2.0 ML of biaxially strained InAs.

formation potential $a_g = a_v + a_c$ is relatively easy to measure by pressure-dependent photoluminescence. Therefore, it is convenient to parametrize a material by a_g and $f \equiv a_c/a_v$, isolating most of the uncertainty in f . Using the fact that for most III-IV semiconductors $a_c/a_v \approx 0.1$,²⁶ a_c and a_g can be estimated even for a material like InAs for which a_c and a_v are not separately known.

Another poorly understood parameter is the unstrained valence-band offset, E_{vbo} defined as $E_v(\text{InAs}) - E_v(\text{GaAs})$ in the absence of strain. The value in Table I is derived using the fact that transition metal impurities are empirically observed to have energy levels fixed with respect to the vacuum, relatively independent of their host environment. Thus, by comparing band edges referenced to the impurity levels in two different materials one deduces the relative band offsets if the strain could be turned off.

III. GEOMETRY DEPENDENCE

The space of all possible island geometries is prohibitively large for analysis. Instead, we consider a subspace: truncated pyramidal islands with (101) type faces and (100) tops, as shown in Fig. 1. The islands are parametrized by the height h , and the base b . The wetting layer was not included in the dot calculation, but the dot energies were compared with quantum well energies corresponding to the wetting

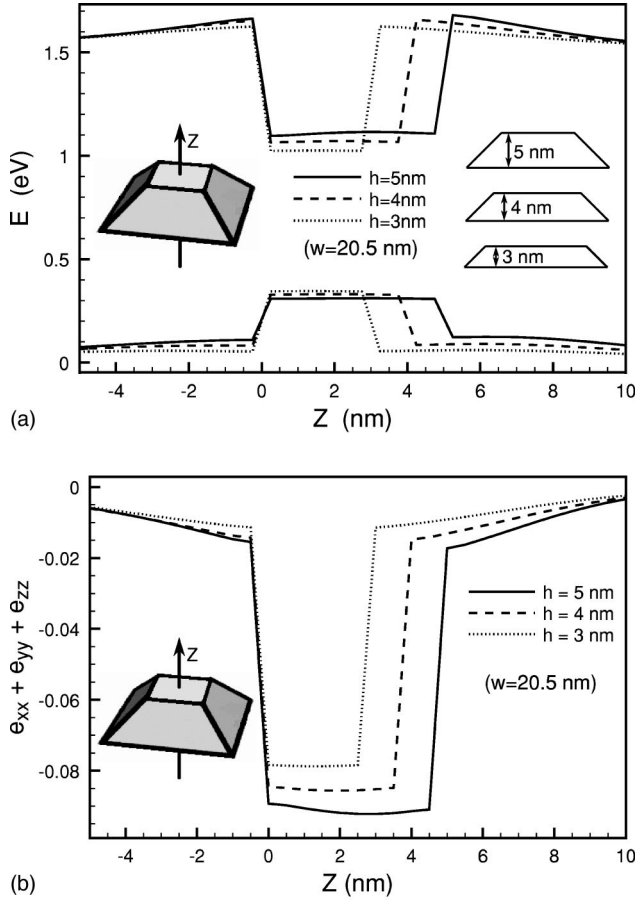


FIG. 2. Effect of height on islands with 20.5 nm bases. (a) Conduction- and valence-band edges along the 100 direction for islands with $h=3, 4,$ or 5 nm. (b) Hydrostatic strain for the same islands.

layer thickness. For consistency, all calculations were done on a grid with a 0.5-nm spacing. This grid spacing has the added benefit that it provides a momentum cutoff of approximately the same magnitude as the underlying crystal lattice. Energies were calculated for $h=3, 4,$ and 5 nm, with b up to 15.5 nm. The minimum values of b were constrained by the requirement that the island have the desired height.

The results are shown in Fig. 1 where single-particle confined state energies are plotted as a function of b (for each of the three heights). It is remarkable that the energies are very insensitive to h . The conduction-band ground state varies by 250 meV over the range $5.5 \text{ nm} \leq b \leq 20.5 \text{ nm}$, but different values of h give energies within 5 meV of each other. The valence-band states vary by ≈ 150 meV as b is changed, but changing h alters the energy by ≤ 10 meV. Intuitively, one expects a strong dependence on h since it determines the smallest confinement size. The resolution of this paradox is found in the strain-induced band structure. Fig. 2(a) shows the conduction-band edges for three dots with the same base, but different heights. A larger value of h corresponds to a more pointy pyramid, resulting in a larger hydrostatic strain near the middle of the island [Fig. 2(b)]. This in turn increases the band gap inside the island, partially compensating the change in confinement energy. Of course the band edges of Fig. 2 give a crude picture of the effect

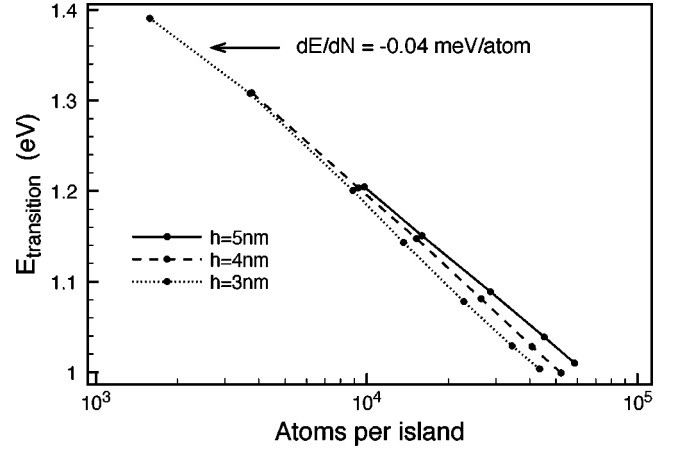


FIG. 3. Exciton recombination energies as a function of island volume, expressed as the total number of atoms in the island.

since the confined state energy depend on band mixing in the full Hamiltonian.

It is also instructive to examine the dependence on island volume. This is shown in Fig. 3 where the ground-state recombination energy is plotted as a function of island volume. The transition energies shown include the exciton binding energy that was computed using the self consistent Hartree approximation, and include the effect of having a different dielectric constant in the barrier and the well. The exciton wave function is assumed to be of the form $\psi^{ij}(\vec{r}_e, \vec{r}_h) = \phi_e^i(\vec{r}_e) \phi_h^j(\vec{r}_h)$ where i and j are band indices. The electron-hole interaction energy is given by

$$V_{eh} = -e \int d^3 r_e |\phi_e(\vec{r}_e)|^2 V_h(\vec{r}_e), \quad (1)$$

$$\vec{\nabla} \cdot [\epsilon(\vec{r}) \vec{\nabla} V_h(\vec{r})] = -4 \pi e |\phi_h(\vec{r})|^2, \quad (2)$$

$$|\phi_{e,h}(\vec{r})|^2 = \sum_{i=1}^8 |\phi_{e,h}^i(\vec{r})|^2. \quad (3)$$

The exciton wave functions were computed by iteratively solving for $\phi_e^i(\vec{r}_e)$ and $\phi_h^j(\vec{r}_h)$ in the potential produced by the other particle. The energies typically converged to within < 0.1 meV in two or three iterations.

The volume is expressed as the number of atoms, $N \approx 8V/a^3$, where V is the island volume, and a^3 is the volume of the GaAs unit cell. (The GaAs unit cell was used since the calculational grid is commensurate with the surrounding GaAs.) Using N serves as a reminder of the small sizes involved, and how close we are to the fundamental size limits. The one insurmountable obstacle to miniaturization of semiconductor nanostructures is atomic scale granularity, which limits both the minimum size of a heterostructure, and the precision with which its dimensions may be specified.

Viewing the results in this way, we see that size matters more than shape. The spread in energies due to different shapes is relatively small compared to the dependence on overall volume, and becomes larger with increasing island volume. For $N=10^4$ the recombination energies span only 20 meV for $3 \text{ nm} \leq h \leq 5 \text{ nm}$, while for $N=4 \times 10^4$ the energies span 40 meV. This reflects the fact that in the smaller

TABLE II. Dependence on material parameters for the ground-state conduction-band energy E_c , ground-state valence-band state E_v , and $E_g = E_c - E_v$. All energies were computed for a $3.8 \text{ nm} \times 6.2 \text{ nm}$ untruncated island.

P	$P dE_c/dP$ (eV)	$P dE_v/dP$ (eV)	$P dE_g/dP$ (eV)
γ_1^L	-0.021	-0.315	0.294
γ_3^L	-0.032	0.215	-0.247
a_g	0.270	0.043	0.227
E_p	0.151	-0.043	0.194
γ_2^L	-0.026	0.123	-0.149
C_{xxyy}	-0.107	0.026	-0.133
E_{gap}	0.137	0.031	0.106
C_{xxxx} (GaAs)	0.069	0.003	0.066
C_{xyxy} (GaAs)	0.061	-0.002	0.063
b	0.0002	0.051	-0.0501
C_{xxyy} (GaAs)	-0.034	-0.002	-0.032
C_{xyxy}	0.018	-0.005	0.023
Δ	-0.016	0.006	-0.022
d	0.0005	0.021	-0.021
E_{vbo}	0.038	0.058	-0.020
f	0.032	0.047	-0.015
C_{xxxx}	-0.007	-0.019	0.012

dots the wave function extends further into the barrier, and hence the shape of the dot is less important. This provides an additional explanation for the insensitivity to h : truncating the pyramid makes a relatively small change in the island's volume.

Recently, photoluminescence measurements have been performed on single InAs/GaAs islands with energies near 1.30 eV.^{29,30} The observed variation across a sample is typically in the range of 1.30 to 1.35 eV, corresponding to $2400 \leq N \leq 4000$ in Fig. 3. Within this energy range the calculated variation due to shape is quite small, indicating that the observed variation is due to size fluctuations. Without a detailed model of island formation, it is difficult to say much about the expected fluctuations in island size. Assuming that the island fluctuations are purely statistical, and are of order $1/\sqrt{N}$, an island with $\langle N \rangle = 3000$ would have fluctuations on the order of $\Delta N \approx 50$ corresponding to ± 1.5 meV. This suggests that the experimentally observed variations in recombination energy are due to variations in island volume beyond simple statistics of the number of atoms, and instead depend on the dynamics of island formation. A successful prediction of the island size distribution would lend credence to a theory of island formation by testing for more than simply the typical island size.

IV. MATERIAL PARAMETER DEPENDENCE

The computed energy levels of a strained quantum dot depend on 35 different material parameters, some of which are known rather accurately (e.g., the elastic constants) while others are not (e.g., the ratio a_v/a_c , as discussed in Sec. II). To obtain good quantitative agreement between theory and experiment we must determine which of the myriad material parameters have the strongest effect on computed energies. To assess the effect of small variations in the parameters, we have computed the derivatives of the single-particle confined

state energies with respect to most of the parameters in Table I. Since we will examine 17 different parameters we will limit consideration to a single island with $h = 3.8$ and $b = 6.2 \text{ nm}$. This size gives an excitonic recombination energy of 1.32 eV (and $E_g = E_c - E_h = 1.366$ eV), in agreement with recent experiments on single dots.

To estimate the sensitivity to small changes in the material parameters, derivatives were computed for most of the InAs parameters, and for the GaAs elastic parameters. The piezoelectric constant e_{14} was omitted since it is responsible for only a small energy shift. The dielectric constant was also omitted since it only affects the exciton binding energy, and we only consider single-particle energies. The GaAs electronic parameters may be ignored since the confined state wave functions fall off rapidly in the GaAs barrier. On the other hand, the GaAs elastic constants are included in the analysis since they cannot be dismissed on such grounds. The strain in the island not only depends on the stiffness of the island material, but also on that of the barrier material against which the island pushes. The derivatives were computed numerically by varying each of the parameters over a range of $\pm 2\%$, and recomputing the electronic energies. Only the lowest conduction-band state, and the highest valence-band state were considered.

The results are shown in Table II. By tabulating PdE/dP one can easily read off the effect of varying a parameter. For example, a fractional change of 0.1 in γ_1^L changes $E_g = E_c - E_v$ by 0.1×0.29 eV. The conduction-band ground state is most sensitive to the gap deformation potential, followed by E_p , and the zero strain gap, E_{gap} , while the valence-band ground state is most sensitive to the Luttinger parameters. The recombination energy is most sensitive to γ_1^L , followed by γ_3^L , and a_g . This is fortuitous since of all the deformation potentials, a_g is known most accurately. The least sensitive parameters are C_{xxxx} , $f = a_c/a_v$, and E_{vbo} . f and E_{vbo}

TABLE III. Approximated elastic constants used in the two-parameter VFF model.

Parameter	InAs	GaAs
C_{xxxx}	8.53×10^{11} dyne/cm ²	12.03×10^{11} dyne/cm ²
C_{xxyy}	4.90×10^{11} dyne/cm ²	5.07×10^{11} dyne/cm ²
C_{xyxy}	3.14×10^{11} dyne/cm ²	5.20×10^{11} dyne/cm ²

happen to be the parameters known with the least certainty, as was discussed in Sec. II.

The insensitivity of E_g to f and E_{vbo} is ultimately a consequence of the islands' strong confinement. Small changes in f or E_{vbo} increase (or decrease) the barrier for the electron at the expense of the hole's barrier. Since both carriers are strongly confined, such redistributions of barrier height have little effect on the difference $E_c - E_v$. The strong sensitivity to the Luttinger parameters is somewhat discouraging since the tabulated values vary depending on the measurement used. This result demonstrates the importance of using identical parameters when comparing different models. Otherwise, one may confuse model dependence for merely using a different set of material parameters.

This analysis assumes, of course, that any deviations from the tabulated parameters are small. Large errors in the assumed value of E_{vbo} can have profound effects on the calculated electronic structure. An example of such a situation is found in GaSb/GaAs islands, for which there is good evidence that the band lineups are significantly different than originally thought.^{31,32} It should be noted that the band lineup in a strained structure depends on the deformation potentials as well as E_{vbo} .

As an example of how these results may be used, we may estimate the error introduced by using the two-parameter VFF to compute the strain. As discussed in Sec. II, the two-parameter VFF cannot reproduce three experimentally determined elastic constants, and hence, only approximates the experimentally determined bulk elastic properties. Given two VFF parameters, however, we can determine the three elastic constants that would be measured for such a material if it existed. The elastic constants corresponding to the two-parameter VFF are shown in Table III. Using the results in Tables II and III, we find that using the VFF elastic parameters gives a shift in the recombination energy of +24 meV.

It is interesting to note that this energy shift may be translated into an equivalent number of atoms using Fig. 3. For the island under consideration ($E_g = 1.37$ eV), a 24 meV shift corresponds to about 500 atoms.

V. CONCLUSIONS

While large-scale quantum-dot calculations using complicated Hamiltonians have become feasible, the results are no better than the input parameters used. The size dependence of the confinement energy is obviously important for interpreting experimental results. Calculations show that contrary to intuition, the complexities of strain make the electronic energies more sensitive to the base of the island than to its height. This is somewhat discouraging for reckoning theory and experiment since one of the best ways of determining the island geometry is atomic force microscopy on islands that have been left uncovered. Due to the size of an AFM tip the lateral resolution is less than the vertical resolution. Hence, the most important geometrical parameter is the one that is most difficult to measure.

Even if the island geometry is precisely known, uncertainties in material parameters may render a calculation inaccurate. It is fortunate that the most sensitive deformation potential, a_g , is the easiest to measure. The two least-well-characterized parameters, E_{vbo} and f are among the least important: a 10% shift in either one changes the recombination energy by about 2 meV. This means that the considerable experimental effort needed to make precise determinations of E_{vbo} and f is not necessary for understanding Stranski-Krastonov islands. Of course we have only addressed the matter of small variations in the parameters. If, for example, E_{vbo} were to have the wrong sign the electronic structure would change dramatically.

If the material parameters are known to better than 10%, then the error in the computed energy should be a few tens of meV. Since this is slightly less than the ≈ 50 meV variation in measured recombination energy it would seem that for comparison with current experiments, determining the island geometry is more important than obtaining more accurate material parameters. On the other hand, these error estimates suggest that for high precision calculations it may well be necessary either to make more precise measurements, or to develop *ab initio* methods capable of providing the necessary data.

*Electronic address: cpryor@thegrid.net

¹J. Y. Marzin and G. Bastard, Solid State Commun. **91**, 39 (1994).

²A. Wojs, P. Hawrylak, S. Fafard, and L. Jacak, Phys. Rev. B **54**, 5604 (1996).

³M. Grundmann, O. Stier, and D. Bimberg, Phys. Rev. B **52**, 11 969 (1995).

⁴M. Grundmann, N. N. Ledentsov, O. Stier, D. Bimberg, V. M. Ustinov, P. S. Kopev, and Z. I. Alferov, Appl. Phys. Lett. **68**, 979 (1996).

⁵M. Grundmann, N. N. Ledentsov, O. Stier, J. Bohrer, D. Bimberg, V. M. Ustinov, P. S. Kopev, and Z. I. Alferov, Phys. Rev. B **53**, R10 509 (1996).

⁶C. Pryor, M.-E. Pistol, and L. Samuelson, Phys. Rev. B **56**, 10 404 (1997).

⁷M. A. Cusack, P. R. Briddon, and M. Jaros, Phys. Rev. B **54**, R2300 (1996).

⁸M. A. Cusack, P. R. Briddon, and M. Jaros, Phys. Rev. B **56**, 4047 (1997).

⁹H. T. Johnson, J. Appl. Phys. **84**, 3714 (1998).

¹⁰H. Jiang and J. Singh, Appl. Phys. Lett. **71**, 3239 (1997).

¹¹H. Jiang and J. Singh, Phys. Rev. B **56**, 4696 (1997).

¹²C. Pryor, Phys. Rev. B **57**, 7190 (1998).

¹³C. Pryor, Phys. Rev. Lett. **80**, 3579 (1998).

¹⁴See MRS Bull. **23** (1998).

¹⁵A. J. Williamson, A. Zunger, and A. Canning, Phys. Rev. B **57**, R4253 (1998).

¹⁶L.-W. Wang and A. Zunger, J. Chem. Phys. **100**, 2394 (1994).

¹⁷J. Kim, L.-W. Wang, and A. Zunger, Phys. Rev. B **57**, R9408 (1998).

- ¹⁸K. Georgsson, N. Carlsson, L. Samuelson, W. Seifert, and L. R. Wallenberg, *Appl. Phys. Lett.* **67**, 2981 (1995).
- ¹⁹M.-E. Pistol, J. O. Bovin, A. Carlsson, N. Carlsson, P. Castrillo, K. Georgsson, D. Hessman, T. Junno, L. Montelius, C. Persson, L. Samuelson, W. Seifert, and L. R. Wallenberg, in *Proceedings of the 23rd International Conference on the Physics of Semiconductors*, edited by M. Scheffler and R. Zimmermann (World Scientific, Singapore, 1996), No. 2, pp. 1317–1320.
- ²⁰H. Lee, W. Yang, R. Lowe-Webb, and P. C. Sercel, in *Proceedings of the 24th International Conference on the Physics of Semiconductors*, edited by D. Gershoni (World Scientific, Singapore, 1998).
- ²¹P. Keating, *Phys. Rev.* **145**, 637 (1966).
- ²²L. D. Landau and E. M. Lifshitz, *Elasticity* (Pergamon, London, 1959).
- ²³C. Pryor, J. Kim, L. W. Wang, A. J. Williamson, and A. Zunger, *J. Appl. Phys.* **83**, 2548 (1998).
- ²⁴T. B. Bahder, *Phys. Rev. B* **41**, 11 992 (1990).
- ²⁵Jane K. Cullum and Ralph A. Willoughby, *Lanczos Algorithms for Large Symmetric Eigenvalue Computations* (Birkhauser, Boston, 1985), Vol. 1-2.
- ²⁶D. D. Nolte, W. Walukiewicz, and E. E. Haller, *Phys. Rev. Lett.* **59**, 501 (1987).
- ²⁷*Numerical Data and Functional Relations in Science and Technology*, edited by O. Madelung, M. Schilz, and H. Weiss, Landolt-Börnstein, New Series, Group III, Vol. 17, Pt. a (Springer-Verlag, New York, 1982).
- ²⁸A. Adachi, *J. Appl. Phys.* **53**, 8775 (1982).
- ²⁹L. Landin, M. S. Miller, M.-E. Pistol, C. Pryor, and L. Samuelson, *Science* **280**, 262 (1998).
- ³⁰E. Dekel, D. Gershoni, E. Ehrenfreund, D. Spektor, J. M. Garcia, and P. M. Petroff, *Phys. Rev. Lett.* **80**, 4991 (1998).
- ³¹M. E. Rubin, H. R. Blank, M. A. Chin, H. Kroemer, and V. Narayanamurti, *Appl. Phys. Lett.* **70**, 1590 (1997).
- ³²S. M. North, P. R. Briddon, M. A. Cusack, and M. Jaros, *Phys. Rev. B* **58**, 12 601 (1998).